Chirality arising from small defects in gold nanoparticle arrays

Brian K. Canfield[1], Sami Kujala[1], Kaisa Laiho[1], Konstantins Jefimovs[2], Jari Turunen[2], and Martti Kauranen[1]

[1]*Institute of Physics, Optics Laboratory, Tampere University of Technology P. O. Box 692, FI-33101 Tampere, Finland*

[2]*Department of Physics, University of Joensuu P. O. Box 111, FI-80101 Joensuu, Finland*

brian.canfield@tut.fi

Abstract: The symmetry of metal nanostructures may be broken by their overall features or small-scale defects. To separate the roles of these two mechanisms in chiral symmetry breaking, we prepare gold nanostructures with chirality occurring on different levels. Linear optical measurements reveal small chiral signatures, whereas the chiral responses from second-harmonic generation are enormous. The responses of all structures are remarkably similar, suggesting that uncontrollable defects play an important role in symmetry breaking.

OCIS codes: (260.5430) Polarization; (190.4720) Optical nonlinearities of condensed matter; (260.3910) Metals, optics of.

References and links

1. H. G. Craighead and G. A. Niklasson, "Characterization and optical properties of arrays of small gold particles," Appl. Phys. Lett. **44**, 1134–1136 (1984).
2. W. Gotschy, K. Vonmetz, A. Leitner, and F. R. Aussenegg, "Optical dichroism of lithographically designed silver nanoparticle films," Opt. Lett. **21**, 1099–1101 (1996).
3. H. Tuovinen, M. Kauranen, K. Jefimovs, P. Vahimaa, T. Vallius, and J. Turunen, "Linear and second-order nonlinear optical properties of arrays of noncentrosymmetric gold nanoparticles," J. Nonlinear Opt. Phys. Mater. **11** 421–432 (2002).
4. D. P. Fromm, A. Sundaramurthy, P. J. Schuck, G. Kino, and W. E. Moerner, "Gap-dependent optical coupling of single "bowtie" nanoantennas resonant in the visible," Nano Lett. **4** 957–961 (2004).
5. T. Atay, J.-H. Song, and A. V. Nurmikko, "Strongly interacting plasmon nanoparticle pairs: from dipole-dipole interaction to conductively coupled regime," Nano Lett. **4**, 1627–1631 (2004).
6. L. A. Sweatlock, S. A. Maier, H. A. Atwater, J. J. Penninkhof, and A. Polman, "Highly confined electromagnetic fields in arrays of strongly coupled Ag nanoparticles," Phys. Rev. B **71**, 235408 (2005).
7. T. Vallius, K. Jefimovs, J. Turunen, P. Vahimaa, and Y. Svirko, "Optical activity in subwavelength-period arrays of chiral metallic particles," Appl. Phys. Lett. **83**, 234–236 (2003).
8. A. Papakostas, A. Potts, D. M. Bagnall, S. L. Prosvirnin, H. J. Coles, and N. I. Zheludev, "Optical manifestations of planar chirality," Phys. Rev. Lett. **90**, 107404 (2003).
9. S. Linden, C. Enkrich, M. Wegener, J. Zhou, T. Koschny, C. M. Soukoulis, "Magnetic response of metamaterials at 100 terahertz," Science **306**, 1351-1353 (2004).
10. T. W. Ebbesen, H. J. Lezec, H. F. Ghaemi, T. Thio, and P. A. Wolff, "Extraordinary optical transmission through sub-wavelength hole arrays," Nature **391**, 667–669 (1998).
11. H. Ditlbacher, J. R. Krenn, B. Lamprecht, A. Leitner, and F. R. Aussenegg, "Spectrally coded optical data storage by metal nanoparticles," Opt. Lett. **25**, 563–565 (2000).
12. K. L. Kelly, E. Coronado, L. L. Zhao, and G. C. Schatz, "The optical properties of metal nanoparticles: the influence of size, shape, and dielectric environment," J. Phys. Chem. B **107**, 668–677 (2003).

#9291 - $15.00 USD Received 27 October 2005; revised 16 January 2006; accepted 16 January 2006

13. B. K. Canfield, S. Kujala, M. Kauranen, K. Jefimovs, T. Vallius, and J. Turunen, "Polarization effects in the linear and nonlinear optical responses of gold nanoparticle arrays," J. Opt. A-Pure Appl. Opt. **7**, 110–117 (2005).
14. V. A. Markel, V. M. Shalaev, E. B. Stechel, W. Kim, and R. L. Armstrong, "Small-particle composites. I. Linear optical properties," Phys. Rev. B **53**, 2425–2436 (1996).
15. V. M. Shalaev, E. Y. Poliakov, and V. A. Markel, "Small-particle composites. II. Nonlinear optical properties," Phys. Rev. B **53**, 2437–2449 (1996).
16. C. Anceau, S. Brasselet, J. Zyss, and P. Gadenne, "Local second-harmonic generation enhancement on gold nanostructures probed by two-photon microscopy," Opt. Lett. **28**, 713–715 (2003).
17. M. I. Stockman, S. V. Faleev, and D. J. Bergman, "Coherent control of femtosecond energy localization in nanosystems," Phys. Rev. Lett. **88**, 067402 (2002).
18. B. K. Canfield, S. Kujala, M. Kauranen, K. Jefimovs, T. Vallius, and J. Turunen, "Remarkable polarization sensitivity of gold nanoparticle arrays," Appl. Phys. Lett. **86**, 183109 (2005).
19. B. K. Canfield, S. Kujala, K. Jefimovs, J. Turunen, and M. Kauranen, "Linear and nonlinear optical responses influenced by broken symmetry in an array of gold nanoparticles," Opt. Express **12**, 5418–5423 (2004), http://oe.osa.org/abstract.cfm?id=81638.
20. B. Lamprecht, A. Leitner, and F. R. Aussenegg, "SHG studies of plasmon dephasing in nanoparticles," Appl. Phys. B **68**, 419–423 (1999).
21. M. Kuwata-Gonokami, N. Saito, Y. Ino, M. Kauranen, K. Jefimovs, T. Vallius, J. Turunen and Y. Svirko, "Giant optical activity in quasi-two-dimensional planar nanostructures," Phys. Rev. Lett. **95**, 227401 (2005).
22. J. J. Maki, M. Kauranen, and A. Persoons, "Surface second-harmonic generation from chiral materials," Phys. Rev. B **51**, 1425–1434 (1995).
23. M. Kauranen, T. Verbiest, S. V. Elshocht, and A. Persoons, "Chirality in surface nonlinear optics," Opt. Mater. **9**, 286–294 (1998).
24. K. Li, M. I. Stockman, and D. J. Bergman, "Self-similar chain of metal nanospheres as an efficient nanolens," Phys. Rev. Lett. **91**, 227402 (2003).
25. S. Zou and G. C. Schatz, "Silver nanoparticle array structures that produce giant enhancements in electromagnetic fields," Chem. Phys. Lett. **403**, 62–67 (2005).
26. K. Kneipp, Y. Wang, H. Kneipp, L. T. Perelman, I. Itzkan, R. R. Dasari, and M. S. Feld, "Single molecule detection using surface-enhanced Raman scattering (SERS)," Phys. Rev. Lett. **78**, 1667–1670 (1997).

1. Introduction

Comprehension of the basic physical processes underlying the optical responses of metal nanoparticles is rapidly increasing. [1, 2, 3, 4, 5] Such particles and arrays thereof are expected to have a multitude of potential applications in topics such as plasmonic waveguides, [6] nanoscale polarization control, [7, 8] negative refractive index materials, [9] and superefficient light transmission. [10] The optical responses are dominated by plasmon resonances that depend on the size, shape, ordering, and dielectric environment of the particles. [3, 11, 12, 13] On the other hand, the plasmon modes tend to concentrate around very small-scale structural features, [14, 15] which can lead to an enormous enhancement of the local field. These features, such as possible defects, can therefore be expected to be disproportionately important in determining the optical responses of the structures, the nonlinear ones in particular. For example, spatially overlapping fundamental and second-harmonic modes have been shown to be favorable for second-harmonic generation (SHG) from nanostructures. [16, 17]

Metal nanoparticle arrays are typically fabricated using electron beam lithography (EBL). EBL techniques continue to evolve, enabling ever more precise control over the overall size, shape, and orientation of the particles. Nevertheless, the fabrication process often produces structural defects such as bumps, pits, and other small-scale structural deviations (within individual particles) observed in scanning electron micrograph (SEM) images of nanoparticles (c.f., Fig. 1 and Refs. [2, 4, 5, 13], etc.)

We have previously investigated the linear and nonlinear properties of arrays of L-shaped metal nanoparticles similar to the one shown in Fig. 1. [13, 18, 19] Such anisotropic particles have a basic noncentrosymmetric shape, which is favorable for the second-order nonlinear response. [20] However, the reflection symmetry of ideal particles is easily broken. This renders the samples chiral and can be observed as shifts in the transmission axes directions, [18] polar-

#9291 - $15.00 USD Received 27 October 2005; revised 16 January 2006; accepted 16 January 2006

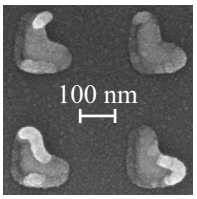

Fig. 1. SEM image of nanoparticles exhibiting defects within individual particles.

ization azimuth rotation, [18] and symmetry-disallowed SHG. [19] Qualitatively, such observations can be explained by assuming otherwise ideal particles but with an asymmetric overall shape. [18] However, the real origin of the chiral symmetry breaking is not yet known.

In this article we show that the small-scale structural defects of the particles play an important role in symmetry breaking. We design and prepare samples where chirality is introduced in three different ways on the overall structure of a nanoparticle array: 1) achiral (achiral particles and achiral ordering); 2) particle-level chirality (chiral particles and achiral ordering); and 3) array-level chirality (achiral particles and chiral ordering). The samples are characterized both by linear optical techniques and by second-harmonic generation. In the linear response, chirality is shown to result in shifted transmission axes and polarization azimuth rotation. Chirality is also expected to lead to a different response for the two circular polarizations, which is not observed in the linear response. The efficiency of SHG, on the other hand, is shown to exhibit a very large difference between the two circular polarizations of the fundamental field. Most importantly, the responses of all three samples are remarkably similar, suggesting that the small-scale defects, over which we have no control and which are significant for the nonlinear response, are indeed a substantial factor in the symmetry breaking.

2. Experiments and discussion

A schematic of the three different arrays of L-shaped nanoparticles studied is depicted in Fig. 2(a). The sample was fabricated using EBL and lift-off techniques. [3] All particles have 100 nm linewidths and gold thickness of 20 nm, and the grating spacing in each array is 400 nm. The arrays are also covered by a 20 nm-thick protective glass layer. Array S1 possesses achiral structure on both the particle and array levels, with symmetric particles (200 nm arm lengths) arranged in a regular square lattice (note that the array in Fig. 1, though fabricated with identical parameters, does not depict S1). A mirror symmetry plane ('*x*') then exists along the axis bisecting the arms of the symmetric L, coincident with the mirror plane for the array (the axes remain fixed with respect to the particle orientation in S1 for all three arrays, which is experimentally convenient). Array S2 exhibits particle-level chirality, where one arm is approximately 30% longer, removing the mirror symmetry plane but maintaining the periodic array structure. S3 features achiral particles in a chiral array structure, the particles having been rotated by 27° relative to S1. Comparison between the arrays should thus provide details about the origins of chirality in these structures.

Basic characterization of the samples was accomplished by measuring their extinction spectra with a white light source and two fiber optic spectrometers (Avantes AvaSpec-2048 and NIR256) covering the combined range of 400 nm to 1700 nm. The spectra in Fig. 2(b) show that the arrays are highly dichroic, with 400 nm separations between *x*- and *y*-polarization resonances, owing to the size and shape of the particles. [2] In addition, the peak locations vary significantly among the three arrays. Previous results have shown that with increasing particle size (closely related to the longer arm in S2), the extinction resonance significantly redshifts. [13]

#9291 - $15.00 USD Received 27 October 2005; revised 16 January 2006; accepted 16 January 2006

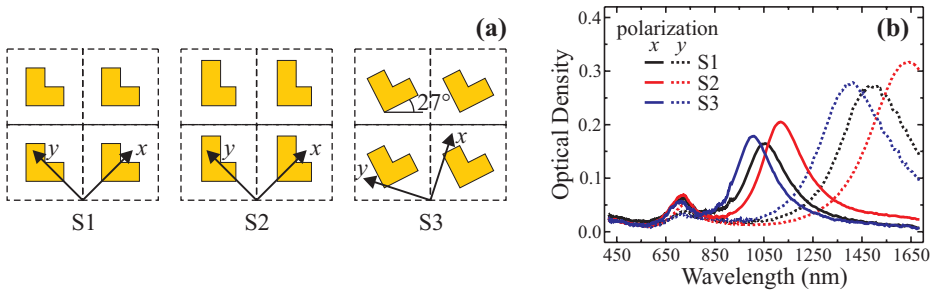

Fig. 2. Nanoparticle array designs and extinction spectra. (a) S1: achiral array of achiral particles; S2: achiral array of chiral particles; S3: chiral array of achiral particles. (b) Extinction spectra for *x*- and *y*-polarizations.

The large blueshifts in the S3 spectra are intriguing, as previously the effect of rotated particles was found to be relatively small ($\sim$ 20 nm). [13] However, the array structures in Ref. [13] were rotated by 45°, preserving the mirror planes of the arrays. The present result suggests that the lack of a symmetry plane in the array structure may exert an even larger influence on the extinction resonance location.

Linear polarization transmission and azimuth rotation measurements were performed on the arrays using a femtosecond (fs) laser (Time-Bandwidth GLX200, $\sim$200 fs pulse duration, 82 MHz repetition rate, central wavelength 1060 nm, 420 mW average power) attenuated to microwatt-range power levels to ensure linearity. [18] The transmittances exhibit angular shifts of the actual transmission axes from the design axes *x* and *y*—11° for S1, −2° for S2, and 6° for S3. Note that the shifts of S1 and S3 are qualitatively similar, in agreement with the similarity of their individual particles. The shift of S2, on the other hand, has a different sign because its asymmetric overall particle shape removes any preferred directions. Azimuth rotation measurements reveal small but equivalent average rotations of $0.6^\circ \pm 0.2^\circ$ for all three arrays. This is significantly more at this wavelength than in our earlier samples, [18] probably indicative of a higher density of biased defects in the present samples. Note also that even larger rotations exceeding 1° have been obtained for chiral gammadion nanostructures. [21] However, these samples were fabricated with ion beam milling to be much thicker (100 nm), and they lack a protective glass overlayer, which can easily explain the differences to the present results. The linear measurements already suggest that all present samples are chiral regardless of design. This, in turn, implies that chirality arises from a source of broken symmetry common to all three arrays, ruling out particle shape and array structure. Unique small defects within individual particles, however, are expected to be present in all arrays similarly, making them likely suspects for symmetry breaking.

Chirality is also expected to lead to different responses for left- and right-hand circularly-polarized light (LHC and RHC, respectively), which is also the cause of the azimuth rotation. To test whether circular-difference effects are present in transmission, we used a setup that was subsequently used for SHG. Both linear transmission and second-harmonic measurements are based on continuous polarization variation (CPV), where the polarization of the fs laser source is varied from linear to circular by a continuously-rotating quarter waveplate (QWP, Fig. 3). Note that the laser is near resonance for the *x*-polarized spectra of Fig. 2(b). The beam (suitably attenuated for the linear measurements) was chopped, polarized with a high-quality calcite polarizer, and moderately focused with a 20 cm focal-length lens. The QWP was then used to modulate the polarization state at the sample. A visible-blocking filter (VIS) preceded the sample to block stray light and SHG from the prior optics. The sample was oriented at

#9291 - $15.00 USD Received 27 October 2005; revised 16 January 2006; accepted 16 January 2006

normal incidence to the beam. The detector was a scatter plate (SP) and photodetector (PD) in the linear case, or an infra-red blocking filter (IR) and an interference filter and photomultiplier tube (PMT) in the SHG experiments. In both versions the detector was connected to a lock-in amplifier referencing the chopper frequency.

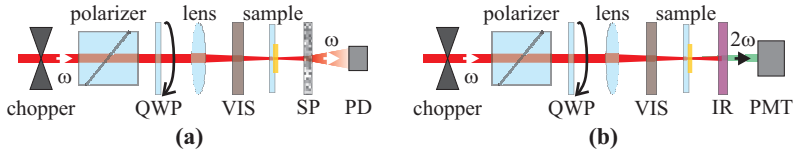

Fig. 3. CPV experimental setups for (a) the linear case, and (b) the SHG case; ω: fundamental beam, 2ω: second-harmonic beam.

Data were acquired by aligning the fast axis of the QWP parallel to the input linear polarization direction ($x-y$). The QWP was then rotated through a full revolution and the intensity as a function of the QWP angle was recorded. A difference in transmitted intensity, I, between LHC and RHC states (i.e., odd multiples of $\pi/4$) then yields a circular-difference response (CDR): [22, 23]

$$\mathrm{CDR} = 2\,\frac{I_{LHC}(\omega) - I_{RHC}(\omega)}{I_{LHC}(\omega) + I_{RHC}(\omega)}\,. \tag{1}$$

This expression is also valid for the SHG intensity at 2ω. A CDR at normal incidence, where sample anisotropy can be disregarded, is therefore a direct indication of chirality.

F-CPV measurements at the fundamental wavelength, however, appear insensitive to the lack of symmetry in the arrays on both the small and large scales, yielding negligible CDR values within uncertainty. The SH-CPV measurements shown in Fig. 4, on the other hand, reveal very large CDR values on the order of 200%. Interestingly, the achiral array S1 demonstrates a substantially greater CDR (175%) than the chiral particle array S2 (140%), while S3 exhibits an exceptional CDR of 180% (uncertainty in these values is $\pm$10%). The variations in the CDR values may be attributed to competition between the large- and small-scale structures of the arrays. Reminiscent of the shifts in the transmission axes, S2's CDR is decreased compared to S1, despite its chiral particles, because the large-scale contribution from longer arms has a different sign compared to the small-scale defect contribution. The magnitude of S3's CDR increases slightly because the array structure contribution has the same sign as the defect contribution.

In addition, similar curve features appear for all three arrays (Fig. 4), suggesting that the larger-scale symmetry properties such as overall particle shape or array structure exert smaller influences on the second-order response as well. This observation also fits with the relative changes in CDR values among the arrays compared to the overall magnitude. As the nonlinear response is expected to be driven primarily by the small defects, which also appear to be the dominant source of broken symmetry, the chiral signatures in the nonlinear response are particularly large.

A compelling case may be made for this conclusion. Theoretical calculations of the local field around small ($\sim$ few nm) structures have predicted large enhancements on the order of 10^4 in field strength near them. [24, 25] Because SHG depends on the square of the input fundamental field, the second-harmonic yield may therefore be increased by many orders of magnitude, making SHG measurements much more sensitive. Recent experimental results have demonstrated immense enhancements ($\sim 10^{14}$) in surface-enhanced Raman scattering yields from single molecules in silver colloidal solutions. [26] SHG also depends strongly on symmetry, so symmetry breaking by defects can be much more striking in the SHG signal than in the fundamental response.

#9291 - $15.00 USD Received 27 October 2005; revised 16 January 2006; accepted 16 January 2006

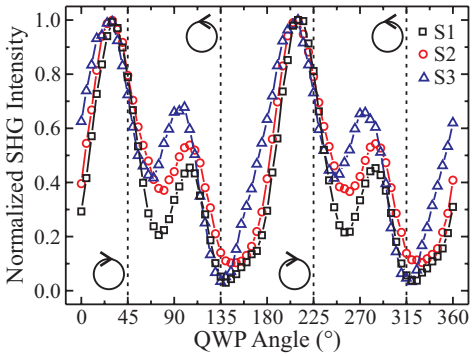

Fig. 4. Results of SH-CPV measurements. The connecting line segments are guides to the eye. The circular polarization states are indicated by vertical dashed lines.

In the present work we have addressed the chiral symmetry breaking of the nanoparticle arrays mainly by the circular-difference response and found that SHG is particularly sensitive to such breaking. However, detailed information about the samples can be obtained from a more complete tensor analysis of the SHG response. In the present experiments where the fundamental beam is applied at normal incidence, the intensity of any second-harmonic signal can be expanded as [22, 23]

$$I_j(2\omega) = \left| f_j E_x^2(\omega) + g_j E_y^2(\omega) + h_j E_x(\omega) E_y(\omega) \right|^2, \tag{2}$$

where f, g, and h are coefficients that characterize the nonlinear response and subscript $j = x, y$. (Note that this expression operates on the level of fields, so it implicitly includes all local and nonlocal contributions and can be applied even to structured arrays of nanoparticles.) It is already evident that circular-difference effects ($E_x = \pm iE_y$) can occur only if f (or g) and h are simultaneously nonvanishing and sufficient phase differences occur between the coefficients. However, for a full tensor analysis of the response, the present CPV measurements need to be combined with polarized detection of second-harmonic light. Such work is underway in our laboratory and we expect its results to be essential in building a connection to any microscopic models of the nonlinear response.

3. Conclusion

We have demonstrated that small-scale defects in gold nanoparticles break the symmetry of the larger-scale particle and array structures and render the arrays chiral. The presence of chirality may not be readily apparent from linear measurements. However, SHG measurements, being far more sensitive to symmetry through local field enhancement near small defects, reveal strong chiral signatures even from an array designed to be achiral. In addition, when comparing achiral and chiral structures, the similarity of the results implies that large-scale properties such as overall particle shape or array structure exert less influence on the optical responses than the small-scale defects within individual particles.

Acknowledgments

K. Jefimovs is currently with the Laboratory for Micro- and Nanotechnology, Paul Scherrer Institut, CH-5232 Villigen PSI, Switzerland. Funding was from the Academy of Finland (grants 102018, 101362, and 205863). The authors thank Hannu Husu for experimental assistance, and Mark Stockman for productive discussions.

#9291 - $15.00 USD Received 27 October 2005; revised 16 January 2006; accepted 16 January 2006